

Speeding up Stochastic Proximal Optimization in the High Hessian Dissimilarity Setting

Elnur Gasanov
KAUST

Peter Richtárik
KAUST

Abstract

Stochastic proximal point methods have recently garnered renewed attention within the optimization community, primarily due to their desirable theoretical properties. Notably, these methods exhibit a convergence rate that is independent of the Lipschitz smoothness constants of the loss function, a feature often missing in the loss functions of modern ML applications. In this paper, we revisit the analysis of the Loopless Stochastic Variance Reduced Proximal Point Method (L-SVRP). Building on existing work, we establish a theoretical improvement in the convergence rate in scenarios characterized by high Hessian dissimilarity among the functions. Our concise analysis, which does not require smoothness assumptions, demonstrates a significant improvement in communication complexity compared to standard stochastic gradient descent.

1 INTRODUCTION

Machine Learning (ML) has become integral to the advancement of modern applications across diverse sectors, including manufacturing (Arinez et al., 2020; Wen et al., 2022), healthcare (Esteva et al., 2019; Maleki Varnosfaderani and Forouzanfar, 2024), finance (Goodell et al., 2021), retail (Oosthuizen et al., 2021), agriculture (Bhat and Huang, 2021), and beyond. This widespread integration arises from machine learning’s capacity to analyze vast amounts of data, identify patterns, and leverage them for predictive insights.

Many machine learning problems admit a rigorous mathematical formulation. A prominent example is Expected Risk Minimization (ERM) (Shalev-Shwartz and Ben-David, 2014), which is mathematically represented as the minimization problem:

$$\min_{x \in \mathbb{R}^d} \left\{ f(x) \stackrel{\text{def}}{=} \frac{1}{n} \sum_{i=1}^n f_i(x) \right\}, \quad (1)$$

where n denotes the number of data points, $x \in \mathbb{R}^d$ represents the model parameters, and $f_i(x)$ is the loss function associated with i -th data point. It is worth noting that the same formulation (1) can be interpreted in the context of Federated Learning (Konečný et al., 2016; Li et al., 2020a), where n refers to the number of clients, and $f_i(x)$ represents the loss function associated with data of client i .

Despite its simple form, problem (1) is an unusual, rich source of research problems, exhibiting a wide variety of properties and providing convergence bounds that depend on the assumptions imposed on f_i (Woodworth and Srebro, 2016). To focus our analysis amid this variability, we rely on two assumptions commonly found in the literature: Hessian similarity and strong convexity.

Assumption 1 (Hessian similarity). *There exists a constant $\delta \geq 0$ such that for all vectors $x, y \in \mathbb{R}^d$, the following inequality holds:*

$$\frac{1}{n} \sum_{i=1}^n \|\nabla f_i(x) - \nabla f_i(y) - [\nabla f(x) - \nabla f(y)]\|^2 \leq \delta^2 \|x - y\|^2. \quad (2)$$

Assumption 2 (Strong convexity). *Each function f_i is μ -strongly convex, meaning that for all vectors $x, y \in \mathbb{R}^d$, the following inequality holds for some $\mu \geq 0$:*

$$f_i(y) \geq f_i(x) + \langle \nabla f_i(x), y - x \rangle + \frac{\mu}{2} \|x - y\|^2. \quad (3)$$

It is worth noting that when $\mu = 0$, this assumption simplifies to the standard definition of convexity.

Assumption 1 captures the similarity condition first introduced by Shamir et al. (2014) (Lemma 1) to analyze the convergence rate of their DANE algorithm for quadratic functions. This assumption was later independently rediscovered in (Szlendak et al., 2022). Furthermore, it serves as a second-order heterogeneity assumption (Woodworth et al., 2023; Mishchenko et al., 2024), which, in some cases, depends on the input data but not on the data labels. Recently, Assumption 1 has gained attention as a potentially advantageous alternative to the often restrictive Lipschitz smoothness assumption in Deep Learning (Zhang et al., 2020;

Goodfellow et al., 2016). The Lipschitz smoothness assumption posits that for all vectors $x, y \in \mathbb{R}^d$, the norm of the difference between gradients is bounded by a constant $L > 0$ multiplied by the distance between x and y :

$$\|\nabla f(x) - \nabla f(y)\| \leq L\|x - y\|.$$

For instance, **SCAFFOLD** (Karimireddy et al., 2020) leveraged Hessian similarity for quadratic functions, eliminating the dependence on the smoothness constant in communication complexity. Subsequently, the **SONATA** algorithm (Sun et al., 2020) extended this result to strongly convex functions. Recent studies have further built upon Assumption 1 in the context of ERM, leading to the development of more efficient and even accelerated algorithms (Kovalev et al., 2022; Khaled and Jin, 2023; Lin et al., 2023; Jiang et al., 2024a,b; Mishchenko et al., 2024).

We emphasize that our analysis does not rely on the assumption of Lipschitz smoothness. Moreover, smoothness directly implies Assumption 1, as demonstrated in the following derivation:

$$\begin{aligned} & \frac{1}{n} \sum_{i=1}^n \|\nabla f_i(x) - \nabla f_i(y) - [\nabla f(x) - \nabla f(y)]\|^2 \\ \stackrel{(26)}{=} & \frac{1}{n} \sum_{i=1}^n \|\nabla f_i(x) - \nabla f_i(y)\|^2 - \|\nabla f(x) - \nabla f(y)\|^2 \\ \leq & \frac{1}{n} \sum_{i=1}^n \|\nabla f_i(x) - \nabla f_i(y)\|^2 \\ \leq & \frac{1}{n} \sum_{i=1}^n L_i^2 \|x - y\|^2, \end{aligned}$$

where the first equality follows from the variance decomposition formula. Here, L_i denotes the smoothness constant of function f_i . Our derivation above implies that $\delta^2 \leq \frac{1}{n} \sum_{i=1}^n L_i^2$. Notably, in the inequality on the third line, we discard the potentially large term $\|\nabla f(x) - \nabla f(y)\|^2$, indicating that δ can, in practice, be much smaller than the smoothness constant. This observation highlights the extra power of our assumption in comparison to the traditional L -smoothness condition.

The strong convexity assumption is a cornerstone in optimization theory and has been widely utilized across numerous algorithms (Nesterov et al., 2018). In particular, this assumption ensures that the function $f(x)$ is μ -strongly convex, guaranteeing the existence of a unique solution $x_* \in \mathbb{R}^d$ to the ERM problem when $\mu > 0$. In the case where $\mu = 0$, x_* refers to any point in $\text{Argmin } f$.

1.1 Contributions

This paper is dedicated to a more in-depth analysis of the Loopless Stochastic Variance Reduced Proximal point method (**L-SVRP**), which was initially introduced in the work of Khaled and Jin (2023), inspired by the **L-SVRG** of Kovalev et al. (2020). Our primary contributions are outlined as follows:

1. Under Assumptions 1 and 2, we derive a novel iteration complexity bound of $O\left(\left(n\frac{\delta}{\mu} + n\right) \log \frac{\|x_0 - x_*\|^2}{\epsilon}\right)$ for the **L-SVRP** algorithm, outlined in Algorithm 3. Importantly, our result demonstrates a significant improvement over the iteration and communication complexity bounds previously established by Khaled and Jin (2023). In particular, our complexity bound is asymptotically sharper in the $\frac{\delta}{\mu} \geq n$ regime, surpassing the earlier results obtained by Khaled and Jin (2023); Richtárik et al. (2024a). Moreover, unlike previous analyses, such as Traoré et al. (2024), our approach does not rely on the smoothness assumption. Additionally, we observe that **L-SVRP** can be applied to monotone inclusion problems, as demonstrated by Sadiev et al. (2024).
2. We provide experimental validation to support our theoretical findings. Specifically, our experiments confirm the linear convergence rate of the **L-SVRP** algorithm and verify the accuracy of the derived upper bounds on its convergence rate.

The remainder of the paper is structured as follows. In Section 2, we guide the reader through a detailed exploration of the significance of loopless methods and proximal algorithms, tracing their development and relevance in optimization. Following this, we introduce the **L-SVRP** algorithm, which belongs to both the loopless and proximal categories. In Section 3, we delve into our novel theoretical contributions, offering a thorough comparison between our results and existing iteration complexity rates. Finally, in Section 4, we provide a thorough presentation of our experimental results.

2 THE IMPORTANCE OF LOOPLESS AND PROXIMAL METHODS IN OPTIMIZATION

We begin by exploring the dual nature—both the advantages and limitations—of early stochastic variance reduction methods, which have played a pivotal role in the development of modern optimization algorithms.

2.1 Stochastic Gradient Descent

A natural approach to solving the ERM problem (1) is to employ the Stochastic Gradient Descent (SGD) (Robbins and Monro, 1951) algorithm. At each iteration k of SGD, the algorithm randomly selects an index $i_k \in \{1, \dots, n\}$ and updates the parameters according to the rule

$$x_{k+1} = x_k - \gamma \nabla f_{i_k}(x_k), \quad (4)$$

where γ is a positive stepsize. A key issue with SGD is its convergence behavior: instead of converging to the exact solution of the finite sum problem (1), it converges to a neighborhood of the optimal solution only. The size of this neighborhood is proportional to the variance of the stochastic gradient and the stepsize γ , while being inversely proportional to the strong convexity parameter μ , as shown by Gower et al. (2019). Consequently, the stepsize γ must be reduced to match the target precision ε , leading to very slow convergence of $\tilde{\mathcal{O}}\left(\frac{\max L_i}{\mu} + \frac{\sigma_*^2}{\mu^2 \varepsilon}\right)$, where $\sigma_*^2 = \frac{1}{n} \sum_{i=1}^n \|\nabla f_i(x_*)\|^2$. To overcome these limitations, variance reduction techniques have been developed, leading to faster convergence rates. A prominent example of such methods is the Stochastic Variance Reduced Gradient (Johnson and Zhang, 2013) algorithm.

2.2 Stochastic Variance Reduced Gradient

Stochastic variance reduced gradient methods, such as SVRG (Johnson and Zhang, 2013), address the limitations of SGD by reducing the variance of stochastic gradient estimates, enabling a significant improvement in convergence speed.

Algorithm 1 SVRG

Input: update frequency $m \in \mathbb{N}$, stepsize $\gamma > 0$, initial iterate $x_0 \in \mathbb{R}^d$, reference point $w_0 \in \mathbb{R}^d$, number of iterations $K \in \mathbb{N}$
for $k = 0, 1, 2, \dots, K - 1$ **do**
 Uniformly at random choose $i_k \in \{1, 2, \dots, n\}$
 $x_{k+1} = x_k - \gamma(\nabla f_{i_k}(x_k) - \nabla f_{i_k}(w_k) + \nabla f(w_k))$
 $w_{k+1} = \begin{cases} x_{k+1} & \text{if } (k+1) \% m = 0, \\ w_k & \text{otherwise.} \end{cases}$
end for
Output: x_K

Unlike SGD, the Stochastic Variance Reduced Gradient (SVRG) method (Johnson and Zhang, 2013), as detailed in Algorithm 1, progressively estimates the gradient shift $\nabla f_i(x_*)$. This adjustment allows SVRG to converge precisely to the solution of the original problem (1) with an iteration complexity of $\tilde{\mathcal{O}}\left(n + \frac{L}{\mu}\right)$, assuming an optimal inner loop size m . This improvement

alone represents a significant acceleration compared to the iteration complexity of full batch gradient descent, which is $\tilde{\mathcal{O}}\left(n \frac{L}{\mu}\right)$.

However, practical implementation introduces challenges. The optimal inner loop size m , as suggested by theoretical analysis, depends on the strong convexity parameter μ , which is often unknown or loosely estimated in real-world scenarios.

This issue was addressed by the introduction of L-SVRG, the loopless variant of SVRG (Kovalev et al., 2020; Hofmann et al., 2015; Konečný and Richtárik, 2015). The key trick is to eliminate the inner loop entirely through randomization.

2.3 Escaping the Loop

Loopless SVRG (L-SVRG), as presented in Algorithm 2, closely resembles the original SVRG algorithm, but eliminates the inner loop by employing a randomized update for the reference point w_k .

Algorithm 2 L-SVRG

Input: probability $p \in (0, 1]$, stepsize $\gamma > 0$, initial iterate $x_0 \in \mathbb{R}^d$, reference point $w_0 \in \mathbb{R}^d$, number of iterations $K \in \mathbb{N}$
for $k = 0, 1, 2, \dots, K - 1$ **do**
 Uniformly at random choose $i_k \in \{1, 2, \dots, n\}$
 $x_{k+1} = x_k - \gamma(\nabla f_{i_k}(x_k) - \nabla f_{i_k}(w_k) + \nabla f(w_k))$
 $w_{k+1} = \begin{cases} x_{k+1} & \text{with probability } p \\ w_k & \text{with probability } 1 - p \end{cases}$
end for
Output: x_K

The iteration complexity of this algorithm, when $p = \frac{1}{n}$, matches that of SVRG with the optimal inner loop size m , resulting in the complexity $\tilde{\mathcal{O}}\left(n + \frac{L}{\mu}\right)$. However, in L-SVRG, the expected inner loop length, $\frac{1}{p}$, depends only on the number of samples or clients n , which enhances its practical applicability. Moreover, the convergence analysis becomes more straightforward and easier to interpret.

The application of the loopless framework extends to several other algorithmic pairs. For example, SARAH (Nguyen et al., 2017) is enhanced by its loopless variant, which incorporates probabilistic mechanism in PAGE (Li et al., 2021) and quantization in MARINA (Gorbunov et al., 2021). Notably, PAGE achieves optimal complexity in smooth non-convex settings. Similarly, the stochastic algorithm ESGDA (Yan et al., 2020), designed for saddle point optimization problems, simplifies to RSGDA (Sebbouh et al., 2022), making the analysis more tractable. Finally, some algo-

gorithms, such as **ADIANA** (Li et al., 2020c), **CANITA** (Li and Richtárik, 2021), and **ANITA** (Li, 2022), were developed solely in their loopless form.

To summarize, the loopless approach offers several advantages for algorithm design,

1. it simplifies the structure of otherwise more complex algorithms,
2. it facilitates a more simplified convergence analysis,
3. it often results in tighter convergence bounds, these bounds are never worse than existing approaches and are sometimes significantly sharper,
4. it is versatile and can be applied across various optimization settings.

2.4 Proximal Algorithms

Proximal algorithms (Parikh and Boyd, 2013; Condat et al., 2023) are a fundamental class of optimization methods, particularly useful for handling non-smooth and composite objective functions. They leverage the concept of the proximity operator, defined via:

$$\text{prox}_g(x) \stackrel{\text{def}}{=} \underset{x' \in \mathbb{R}^d}{\text{argmin}} \left\{ g(x') + \frac{1}{2} \|x' - x\|^2 \right\}, \quad (5)$$

where $g : \mathbb{R}^d \rightarrow \mathbb{R} \cup \{+\infty\}$ is an extended real-valued function. If $g(x)$ is a proper, closed, convex function, then the minimizer of $g(x') + \frac{1}{2} \|x' - x\|^2$ exists and is unique (Bauschke and Combettes, 2011). Moreover, if g is differentiable, the following equivalence holds:

$$y = \text{prox}_{\gamma g}(x) \Leftrightarrow y + \gamma \nabla g(y) = x. \quad (6)$$

Further properties and formal statements regarding the proximity operator are provided in the appendix.

The simplest stochastic proximal algorithm is the Stochastic Proximal Point Method (**SPPM**) by Asi and Duchi (2019). At each iteration k , for a randomly selected $i_k \in \{1, \dots, n\}$, the following update is performed:

$$x_{k+1} = \text{prox}_{\gamma f_{i_k}}(x_k), \quad (7)$$

or equivalently, using (6):

$$x_{k+1} = x_k - \gamma \nabla f_{i_k}(x_{k+1}). \quad (8)$$

When compared to (4), we observe that **SPPM** is virtually identical to **SGD**, with one seemingly minor yet conceptual difference: the gradient is computed at the new point x_{k+1} . Proximal algorithms, including **SPPM**, are implicit methods, meaning the update involves solving an equation where the new iterate appears on both

sides. This implicitness leads to enhanced stability in practice (Ryu and Boyd, 2016), drawing parallels with the stability observed in implicit numerical solutions of ordinary differential equations (Griffiths and Higham, 2010). Moreover, the convergence of proximal algorithms does not depend on the smoothness properties of the minimized functions (Richtárik et al., 2024b), which makes them appealing for optimizing deep learning loss objectives where the smoothness assumption may not hold (Zhang et al., 2020).

In recent years, there has been growing interest in applying proximal algorithms within Federated Learning (FL). **FedAvg** (Konečný et al., 2016; McMahan et al., 2017), a well-known FL algorithm used in real-world applications, operates as follows: a client, upon receiving an iterate x_k from the server, performs *several* steps of **SGD** on its local data. The final iterate is then transmitted back to the server for aggregation, and this process repeats iteratively. Performing multiple local iterations can be viewed as approximating the proximal operator applied to the local objective function, akin to solving problem (5) for some surrogate local function. Some researchers propose replacing local steps with the proximity operator to deepen our understanding of local methods and obtain faster convergence rates (Li et al., 2020b; T. Dinh et al., 2020; Jhunjunwala et al., 2023; Li et al., 2024). Other researchers interpret the aggregation step as a proximity operator, achieving state-of-the-art communication complexity for this class of methods (Mishchenko et al., 2022; Grudzień et al., 2023; Hu and Huang, 2023; Malinovsky et al., 2022).

Based on our discussion, we can summarize the key points as follows:

1. Proximal algorithms are particularly relevant in Federated Learning, owing to their connection with local computations and distributed aggregation schemes.
2. They exhibit enhanced stability in practice, particularly in stochastic settings.
3. Their convergence does not rely on smoothness assumptions, making them suitable for nonsmooth optimization problems.

2.5 Loopless and Proximal

Motivated by the reasons outlined in the previous two sections, we focus our research on an algorithm that lies at the intersection of both loopless and proximal methods: the Loopless Stochastic Variance Reduced Proximal Point method (**L-SVRP**).

L-SVRP can be viewed as the implicit counterpart of the previously discussed **L-SVRG** algorithm. Specifically,

Algorithm 3 L-SVRP

Input: probability $p \in (0, 1]$, stepsize $\gamma > 0$, initial iterate $x_0 \in \mathbb{R}^d$, reference point $w_0 \in \mathbb{R}^d$, number of iterations $K \in \mathbb{N}$

for $k = 0, 1, 2, \dots, K - 1$ **do**

Uniformly at random choose $i_k \in \{1, 2, \dots, n\}$

$x_{k+1} = \text{prox}_{\gamma f_{i_k}}(x_k + \gamma(\nabla f_{i_k}(w_k) - \nabla f(w_k)))$

$w_{k+1} = \begin{cases} x_{k+1} & \text{with probability } p \\ w_k & \text{with probability } 1 - p \end{cases}$

end for

Output: x_K

the main update steps of both algorithms are related as follows:

$$x_{k+1} \stackrel{\text{Alg. 2}}{=} x_k - \gamma(\nabla f_{i_k}(x_k) - \nabla f_{i_k}(w_k) + \nabla f(w_k)),$$

$$x_{k+1} \stackrel{\text{Alg. 3}}{=} x_k - \gamma(\nabla f_{i_k}(x_{k+1}) - \nabla f_{i_k}(w_k) + \nabla f(w_k)),$$

where, in deriving the main update rule of Algorithm 3, we utilize the equivalence from (6). This relationship highlights that **L-SVRP** incorporates the gradient at the future iterate x_{k+1} in its update rule, making it an implicit method. In contrast, **L-SVRG** uses the gradient at the current iterate x_k , characterizing it as an explicit method.

Although several alternative algorithms, such as **SVRS** (Lin et al., 2023) and **SABER** (Mishchenko et al., 2024), have recently been proposed—employing similar combinations of loopless and proximal ideas and achieving superior convergence rates under Assumption 1—we wish to emphasize that the goal of this work is to improve the convergence rate of the existing **L-SVRP** algorithm. To the best of our knowledge, we are the first to revisit the theoretical analysis of **L-SVRP**. Other algorithms, such as **RandProx** (Condat and Richtárik, 2023), while sharing similar properties, are analyzed under the assumption of smoothness.

3 THEORETICAL ANALYSIS

To establish contraction, we define a Lyapunov function that combines two components: $\mathbb{E}[\|x_k - x_*\|^2]$ and $\mathbb{E}[\|w_k - x_k\|^2]$. Specifically, we express it as:

$$\Lambda_k := \|x_k - x_*\|^2 + c\|w_k - x_k\|^2,$$

where $c > 0$ is a positive scalar determined later, x_k and w_k are the iterates of Algorithm 3, and $x_* \in \text{Argmin } f$ represents any solution to problem (1).

In the course of our derivations, we will make use of the following conditional expectation:

$$\bar{x}_{k+1} = \mathbb{E}[x_{k+1} \mid x_k, w_k].$$

3.1 Bounding the First Term of the Lyapunov Function

To begin the analysis, we establish a bound $\mathbb{E}[\|x_k - x_*\|^2]$, as presented in Lemma 1.

Lemma 1. *Let Assumption 2 (strong convexity) hold. Let us define $\psi_i(x) \stackrel{\text{def}}{=} f_i(x) - f(x)$. Then, for one iteration of Algorithm 3, the following inequality holds:*

$$\begin{aligned} \mathbb{E}[\|x_{k+1} - x_*\|^2 \mid x_k, w_k] &\leq \frac{1}{1 + \mu\gamma} \|x_k - x_*\|^2 \\ &- \mathbb{E}[\|x_{k+1} - \bar{x}_{k+1}\|^2] - \frac{1}{1 + \mu\gamma} \|\bar{x}_{k+1} - x_k\|^2 \\ &- \frac{2}{\mu + \frac{1}{\gamma}} \mathbb{E}[\langle \nabla \psi_{i_k}(\bar{x}_{k+1}) - \nabla \psi_{i_k}(w_k), x_{k+1} - \bar{x}_{k+1} \rangle \mid x_k, w_k]. \end{aligned} \quad (9)$$

We defer the proof of this lemma to the appendix.

The most challenging term on the right-hand side of inequality (9) is the last inner product. Utilizing Assumption 1, we can bound this term by a quantity proportional to $\|w_k - \bar{x}_{k+1}\|^2$. To eliminate this term in our combined Lyapunov analysis, we introduce Lemma 2, which provides a compensating term that cancels this quantity.

3.2 Bounding the Second Term of the Lyapunov Function

To complement the analysis, we derive a bound for the second term in the Lyapunov function, $\mathbb{E}[\|w_{k+1} - x_{k+1}\|^2]$.

Lemma 2. *For the iterates of Algorithm 3, and for any $\xi \in [0, 1]$ and $\zeta > 0$, the following inequality holds:*

$$\begin{aligned} \mathbb{E}[\|w_{k+1} - x_{k+1}\|^2 \mid x_k, w_k] &\leq (1 - p(1 - \xi))(1 + \zeta)\|w_k - x_k\|^2 \\ &+ (1 - p(1 - \xi))(1 + \zeta^{-1})\|x_k - \bar{x}_{k+1}\|^2 \quad (10) \\ &- p\xi\|w_k - \bar{x}_{k+1}\|^2 \\ &+ (1 - p)\mathbb{E}[\|\bar{x}_{k+1} - x_{k+1}\|^2 \mid x_k, w_k]. \end{aligned}$$

Proof. The proof follows directly. Consider that

$$\begin{aligned} \mathbb{E}[\|w_{k+1} - x_{k+1}\|^2 \mid x_{k+1}, x_k, w_k] &= p\|x_{k+1} - x_{k+1}\|^2 + (1 - p)\|w_k - x_{k+1}\|^2 \quad (11) \\ &= (1 - p)\|w_k - x_{k+1}\|^2. \end{aligned}$$

The remainder involves a series of straightforward

bounds and expansions, as detailed below:

$$\begin{aligned}
 & \mathbb{E} [\|w_{k+1} - x_{k+1}\|^2 | x_k, w_k] \\
 &= \mathbb{E} [\mathbb{E} [\|w_{k+1} - x_{k+1}\|^2 | x_{k+1}, x_k, w_k] | x_k, w_k] \\
 &= (1-p)\mathbb{E} [\|w_k - x_{k+1}\|^2 | x_k, w_k] \\
 &= (1-p)\mathbb{E} [\|w_k - \bar{x}_{k+1} + \bar{x}_{k+1} - x_{k+1}\|^2 | x_k, w_k] \\
 &= (1-p) \left[\|w_k - \bar{x}_{k+1}\|^2 + \mathbb{E} [\|\bar{x}_{k+1} - x_{k+1}\|^2 | x_k, w_k] \right. \\
 &\quad \left. + 2\mathbb{E} [\langle w_k - \bar{x}_{k+1}, \bar{x}_{k+1} - x_{k+1} \rangle | x_k, w_k] \right], \tag{12}
 \end{aligned}$$

where the first equality follows from the tower property, and the second equality is obtained using (11).

Noting that, due to the linearity of expectation and the definition $\bar{x}_{k+1} = \mathbb{E} [x_{k+1} | x_k, w_k]$, we have

$$\begin{aligned}
 & \mathbb{E} [\langle w_k - \bar{x}_{k+1}, \bar{x}_{k+1} - x_{k+1} \rangle | x_k, w_k] \\
 &= \langle w_k - \bar{x}_{k+1}, \mathbb{E} [\bar{x}_{k+1} - x_{k+1} | x_k, w_k] \rangle \tag{13} \\
 &= \langle w_k - \bar{x}_{k+1}, 0 \rangle = 0.
 \end{aligned}$$

Substituting this equality into (12), we obtain

$$\begin{aligned}
 & \mathbb{E} [\|w_{k+1} - x_{k+1}\|^2 | x_k, w_k] \\
 \stackrel{(12)+(13)}{=} & (1-p) [\|w_k - \bar{x}_{k+1}\|^2 \\
 & + \mathbb{E} [\|\bar{x}_{k+1} - x_{k+1}\|^2 | x_k, w_k]] \\
 = & (1-p(1-\xi)) \|w_k - \bar{x}_{k+1}\|^2 \\
 & - p\xi \|w_k - \bar{x}_{k+1}\|^2 \\
 & + (1-p)\mathbb{E} [\|\bar{x}_{k+1} - x_{k+1}\|^2 | x_k, w_k] \\
 = & (1-p(1-\xi)) \|w_k - x_k + x_k - \bar{x}_{k+1}\|^2 \\
 & - p\xi \|w_k - \bar{x}_{k+1}\|^2 \\
 & + (1-p)\mathbb{E} [\|\bar{x}_{k+1} - x_{k+1}\|^2 | x_k, w_k] \\
 \leq & (1-p(1-\xi))(1+\zeta) \|w_k - x_k\|^2 \\
 & + (1-p(1-\xi))(1+\zeta^{-1}) \|x_k - \bar{x}_{k+1}\|^2 \\
 & - p\xi \|w_k - \bar{x}_{k+1}\|^2 \\
 & + (1-p)\mathbb{E} [\|\bar{x}_{k+1} - x_{k+1}\|^2 | x_k, w_k].
 \end{aligned}$$

In the final inequality, we utilize the fact that for any vectors $a, b \in \mathbb{R}^d$ and any constant $\zeta > 0$, the following bound holds: $\|a + b\|^2 \leq (1+\zeta)\|a\|^2 + (1+\zeta^{-1})\|b\|^2$. This concludes the proof. \square

The compensating term $-p\xi\|w_k - \bar{x}_{k+1}\|^2$ comes at the cost of two additional terms. By comparing equations (9) and (10), we observe that many terms cancel each other out. This cancellation is the main idea underlying Theorem 1.

3.3 Combined Lyapunov Analysis

With the bounds established for the individual components of the Lyapunov function, we now combine these results to derive the overall contraction property.

Theorem 1. *Let Assumptions 1 (Hessian similarity) and 2 (strong convexity) hold. For a given $\xi \in [0, 1]$ and constants $c > 0$, $\gamma > 0$, and $\zeta > 0$, suppose the following inequalities are satisfied:*

$$c \leq \frac{1}{(1+\mu\gamma)(1-p(1-\xi))(1+\zeta^{-1})}, \tag{14}$$

$$cp\xi \geq \frac{\delta^2}{\left(\mu + \frac{1}{\gamma}\right)^2 (1-c(1-p))}, \tag{15}$$

$$1-r = (1-p(1-\xi))(1+\zeta) \tag{16}$$

where r is a positive constant, and $p \in (0, 1]$ is the probability parameter from Algorithm 3.

Then, the iterates satisfy:

$$\mathbb{E} [\Lambda_{k+1}] \leq \max \left\{ \frac{1}{1+\mu\gamma}, 1-r \right\} \mathbb{E} [\Lambda_k].$$

The proof is deferred to the appendix.

3.4 Interpretation of Results

While Theorem 1 may initially appear to impose numerous conditions, many of these can be addressed in a straightforward and natural manner. To clarify this, we offer the following corollary, which simplifies and resolves several of these conditions.

Corollary 1. *Let Assumption 1 (Hessian similarity) and Assumption 2 (strong convexity) hold. Further, choose $\gamma > 0$ and $p \in (0, 1]$ such that*

$$\left[\frac{2(3-p)^2}{p^2(p+1)} \right] \delta^2 \gamma^2 \leq 1 + \mu\gamma. \tag{17}$$

Then, for iterates of Algorithm 3, it holds that

$$\mathbb{E} [\|x_K - x_*\|^2] \leq \max \left\{ \frac{1}{1+\mu\gamma}, 1 - \frac{p}{4} \right\}^K \|x_0 - x_*\|^2. \tag{18}$$

Proof. In the context of Theorem 1, we specify

$$c = \frac{2p}{(3-p)^2} \frac{1}{1+\mu\gamma}, \quad \xi = \frac{1}{2}, \quad r = \frac{p}{4}. \tag{19}$$

We now verify that this value of c meets the conditions outlined in Theorem 1. The corresponding value of ζ is obtained via Equation (16):

$$\begin{aligned}
 1 - \frac{p}{4} & \stackrel{(16)+(19)}{=} \left(1 - \frac{p}{2}\right) (1+\zeta) \\
 &= 1 - \frac{p}{2} + \zeta \left(1 - \frac{p}{2}\right) \Leftrightarrow \\
 \frac{p}{4} &= \zeta \left(1 - \frac{p}{2}\right) \Leftrightarrow \\
 \zeta &= \frac{p}{4-2p}. \tag{20}
 \end{aligned}$$

Drawing from (14), we obtain the following expression, which simplifies the inequality for easier interpretation:

$$\begin{aligned}
 c &\stackrel{(14)}{\leq} \frac{1}{(1 + \mu\gamma)(1 - p(1 - \xi))(1 + \zeta^{-1})} \\
 &\stackrel{(19)}{=} \frac{1}{(1 + \mu\gamma) \left(1 - \frac{p}{2}\right) (1 + \zeta^{-1})} \\
 &\stackrel{(20)}{=} \frac{1}{(1 + \mu\gamma) \left(1 - \frac{p}{2}\right) \left(\frac{4}{p} - 1\right)} \\
 &= \frac{2p}{(1 + \mu\gamma)(p^2 - 6p + 8)}.
 \end{aligned}$$

We proceed to verify that

$$c \stackrel{(19)}{=} \frac{2p}{(3-p)^2} \frac{1}{1 + \mu\gamma} \leq \frac{2p}{(1 + \mu\gamma)(p^2 - 6p + 8)}.$$

Given that $p \in [0, 1]$, the following chain of inequalities holds:

$$\begin{aligned}
 c &\stackrel{(19)}{=} \frac{2p}{(3-p)^2} \frac{1}{1 + \mu\gamma} \\
 &\leq \frac{2}{(3-p)^2} \frac{1}{1 + \mu\gamma} \leq \frac{2}{4} \frac{1}{1 + \mu\gamma} \leq \frac{1}{2}.
 \end{aligned} \tag{21}$$

The final step is to confirm that the stepsize condition given in (17) is sufficient to satisfy the remaining condition (15):

$$\begin{aligned}
 &\frac{\delta^2}{\left(\mu + \frac{1}{\gamma}\right)^2} \stackrel{(15)}{\leq} \frac{1}{2} cp(1 - c(1 - p)) \\
 &\stackrel{(21)}{\Leftrightarrow} \frac{\delta^2}{\left(\mu + \frac{1}{\gamma}\right)^2} \leq \frac{1}{4} cp(p + 1) \\
 &\stackrel{(19)}{\Leftrightarrow} \frac{\delta^2 \gamma^2}{(1 + \mu\gamma)^2} \leq \frac{p^2(p + 1)}{2(3 - p)^2} \frac{1}{1 + \mu\gamma} \\
 &\Leftrightarrow \delta^2 \gamma^2 \leq \left[\frac{p^2(p + 1)}{2(3 - p)^2} \right] (1 + \mu\gamma) \\
 &\Leftrightarrow \left[\frac{2(3 - p)^2}{p^2(p + 1)} \right] \delta^2 \gamma^2 \leq 1 + \mu\gamma.
 \end{aligned}$$

Unrolling the contraction recurrence, we finish the proof. \square

We also note a similar result can be obtained for convex functions.

Corollary 2. *Let Assumption 1 (Hessian similarity) and Assumption 2 with $\mu = 0$ (convexity) hold. Let us denote $x_* \in \text{Argmin } f$ and $f^* \stackrel{\text{def}}{=} \min_{x \in \mathbb{R}^d} f(x)$. Choose $\gamma > 0$ and $p \in (0, 1]$ such that*

$$\left[\frac{2(3 - p)^2}{p^2(p + 1)} \right] \delta^2 \gamma^2 \leq 1 + \mu\gamma. \tag{22}$$

Then, for iterates of Algorithm 3, it holds that

$$\frac{1}{K} \sum_{k=1}^K \mathbb{E} [f(\bar{x}_k)] - f^* \leq \frac{\|x_0 - x_*\|^2}{2\gamma K}. \tag{23}$$

The final step involves specifying an appropriate stepsize γ and deriving the corresponding iteration complexity estimate. This is addressed in Corollary 3, with the proof deferred to the appendix.

Corollary 3. *Let Assumptions 1 (Hessian similarity) and 2 (strong convexity) hold. Define the condition number κ as $\kappa \stackrel{\text{def}}{=} \frac{\delta}{\mu}$. If the stepsize is chosen as*

$$\gamma = \frac{1}{\delta} \frac{p}{3 - p} \sqrt{\frac{p + 1}{2}} = \Theta\left(\frac{p}{\delta}\right), \tag{24}$$

and the number of iterations of Algorithm 3 satisfies

$$\begin{aligned}
 K &\geq \left(1 + \frac{1}{p} \left(\frac{3\delta}{\mu} + 4\right)\right) \log\left(\frac{\|x_0 - x_*\|^2}{\varepsilon}\right) \\
 &= \tilde{O}\left(\frac{\kappa + 1}{p}\right),
 \end{aligned}$$

then the following bound holds:

$$\mathbb{E} [\|x_K - x_*\|^2] \leq \varepsilon.$$

Remark 2. *When $p = \frac{1}{n}$, we obtain the iteration complexity*

$$O\left((n\kappa + n) \log \frac{\|x_0 - x_*\|^2}{\varepsilon}\right).$$

Compared to the original complexity $\tilde{O}(\kappa^2 + n)$ by Khaled and Jin (2023), our result is better when $\kappa \geq n$.

Remark 3. *As noted by Khaled and Jin (2023), in the communication model discussed in their paper, the iteration complexity and communication complexity of L-SVRP are asymptotically the same.*

4 EXPERIMENTS

To evaluate the tightness of our theoretical convergence rate, we conduct experiments across a grid of 48 parameter configurations. Specifically, we vary the number of functions n among the set $\{10, 25, 50, 100, 250, 500\}$ and adjust the Hessian heterogeneity parameter δ^2 over eight values exponentially increasing from 10^0 to 10^7 . Due to the stochastic nature of the data generation process, we do not obtain fixed values of δ^2 for each setting; however, the generated values are approximately similar across runs.

For our experiments, we utilize an internal computational cluster node equipped with 10 CPUs. The

code is implemented in Python and leverages standard libraries, including Numpy (Harris et al., 2020) and Scipy (Virtanen et al., 2020).

We perform our tests on quadratic functions defined as follows:

$$f_i(x) = \frac{1}{2}x^\top \mathbf{A}_i x + b_i^\top x, \quad (25)$$

where each $\mathbf{A}_i \in \mathbb{S}_{++}^d$ is a symmetric positive definite matrix of dimension d , and $b_i \in \mathbb{R}^d$ is a vector of the same dimension. In all experiments, we set $d = 100$. For the sake of simplicity, we set $\frac{1}{n} \sum_{i=1}^n b_i = 0$. It is important to note, however, that this simplification prevents the interpolation regime from being satisfied.

By Assumption 1, if the parameter δ^2 exists, it can be explicitly expressed as follows:

$$\delta^2 = \sup_{\substack{x, y \in \mathbb{R}^d \\ x \neq y}} \frac{\sum_{i=1}^n \|\nabla f_i(x) - \nabla f_i(y) - \nabla f(x) + \nabla f(y)\|^2}{\|x - y\|^2}.$$

We demonstrate that, for the quadratic problem (25), this quantity is finite:

$$\begin{aligned} & \sup_{\substack{x, y \in \mathbb{R}^d \\ x \neq y}} \frac{\frac{1}{n} \sum_{i=1}^n \|\nabla f_i(x) - \nabla f_i(y) - \nabla f(x) + \nabla f(y)\|^2}{\|x - y\|^2} \\ &= \sup_{\substack{x, y \in \mathbb{R}^d \\ x \neq y}} \frac{\frac{1}{n} \sum_{i=1}^n \|\mathbf{A}_i(x - y) - \bar{\mathbf{A}}(x - y)\|^2}{\|x - y\|^2} \\ &= \sup_{\substack{x, y \in \mathbb{R}^d \\ x \neq y}} \frac{\frac{1}{n} \sum_{i=1}^n \|(\mathbf{A}_i - \bar{\mathbf{A}})(x - y)\|^2}{\|x - y\|^2} \\ &= \sup_{\substack{z \in \mathbb{R}^d \\ z \neq 0}} \frac{\frac{1}{n} \sum_{i=1}^n \|(\mathbf{A}_i - \bar{\mathbf{A}})z\|^2}{\|z\|^2} \\ &= \sup_{\substack{z \in \mathbb{R}^d \\ z \neq 0}} \frac{z^\top \left[\frac{1}{n} \sum_{i=1}^n (\mathbf{A}_i - \bar{\mathbf{A}})^\top (\mathbf{A}_i - \bar{\mathbf{A}}) \right] z}{\|z\|^2}, \end{aligned}$$

where, in the second equality, we omit the terms b_i and b as they cancel out, thereby saving space in the paper.

Recalling that all matrices under consideration are symmetric, we have:

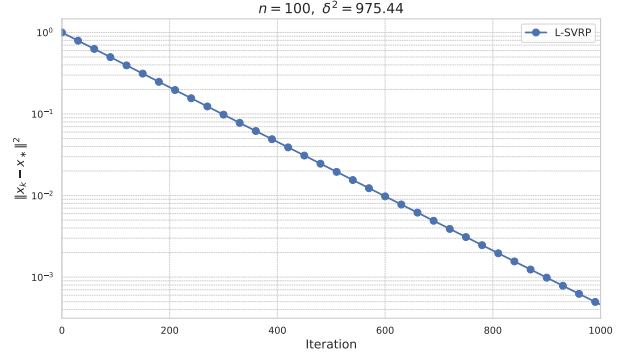


Figure 1: Convergence of **L-SVRP** under one of the 48 configurations examined, where the number of functions $n = 100$ and the Hessian similarity parameter $\delta^2 = 975.44$. As predicted by theoretical analysis, the convergence is linear. We aggregate the slopes from such figures to produce Figure 2.

$$\begin{aligned} \delta^2 &= \sup_{x \in \mathbb{R}^d} \frac{z^\top \left[\frac{1}{n} \sum_{i=1}^n (\mathbf{A}_i - \bar{\mathbf{A}})^\top (\mathbf{A}_i - \bar{\mathbf{A}}) \right] z}{\|z\|^2} \\ &= \sup_{x \in \mathbb{R}^d} \frac{z^\top \left[\frac{1}{n} \sum_{i=1}^n (\mathbf{A}_i - \bar{\mathbf{A}})(\mathbf{A}_i - \bar{\mathbf{A}}) \right] z}{\|z\|^2} \\ &= \sup_{x \in \mathbb{R}^d} \frac{z^\top \left[\frac{1}{n} \sum_{i=1}^n \mathbf{A}_i^2 - \bar{\mathbf{A}}^2 \right] z}{\|z\|^2} \\ &= \left\| \frac{1}{n} \sum_{i=1}^n \mathbf{A}_i^2 - \bar{\mathbf{A}}^2 \right\|, \end{aligned}$$

where $\bar{\mathbf{A}}$ represents the average matrix $\frac{1}{n} \sum_{i=1}^n \mathbf{A}_i$, and the final equality follows from the definition of the matrix spectral norm. Consequently, for quadratic problems, the parameter

$$\delta^2 = \left\| \frac{1}{n} \sum_{i=1}^n \mathbf{A}_i^2 - \bar{\mathbf{A}}^2 \right\|$$

is finite and well-defined. This result was previously established in (Szlendak et al., 2022).

To generate the matrices \mathbf{A}_i , we create random orthogonal matrices \mathbf{Q}_i and random diagonal matrices whose diagonal entries are uniformly sampled from the interval $[1, s]$. The parameter s varies over the set $\{5, 10, 50, 100, 500, 1000, 5000, 10000\}$. This generation process ensures that the strong convexity assumption holds with a constant $\mu = 1$, while allowing δ^2 to range from relatively small to large values.

For each configuration, we run the **L-SVRP** algorithm for 1,000 iterations, repeating this process 200 times to average the squared distances $\|x_k - x_*\|^2$, thereby

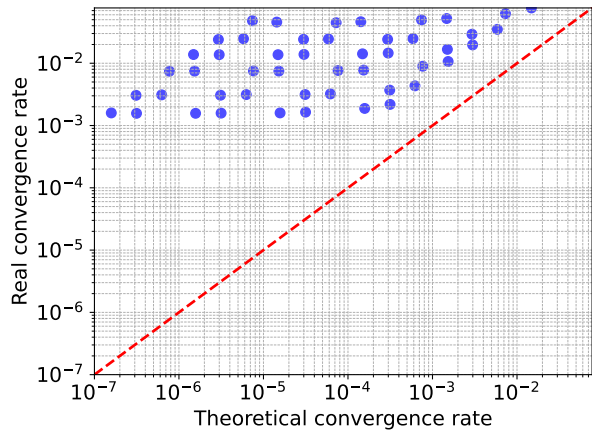


Figure 2: Comparison of real convergence rate vs. theoretical convergence rate. Each point represents one of the 48 problem instances evaluated across varying values of n and δ^2 . The red dashed line denotes the identity line $y = x$. The fact that all points lie above this line confirms the validity of our theoretical analysis. However, the empirical convergence rates are often significantly better than the theoretical predictions, indicating that the theoretical bounds may be further tightened.

approximating the expectation $\mathbb{E}[\|x_k - x_*\|^2]$. The stepsize is defined as in Equation (24). As detailed in the appendix and illustrated in Figure 1, the dynamics of $\log \|x_k - x_*\|^2$ exhibit linear behavior, which is consistent with our theoretical predictions. We consider $1 - x$, where x is the slope of the aforementioned plot, as the empirical convergence rate and compare this value against the theoretical rate, reported in Equation (18). Our results are presented in Figure 2. As observed, the empirical convergence closely aligns with the theoretical predictions. However, since the real convergence rate is often significantly better than the theoretical estimate, this suggests that there may be potential for further improvements in the analysis.

References

- Arinez, J. F., Chang, Q., Gao, R. X., Xu, C., and Zhang, J. (2020). Artificial intelligence in advanced manufacturing: Current status and future outlook. *Journal of Manufacturing Science and Engineering*, 142(11):110804.
- Asi, H. and Duchi, J. C. (2019). Stochastic (approximate) proximal point methods: Convergence, optimality, and adaptivity. *SIAM Journal on Optimization*, 29(3):2257–2290.
- Bauschke, H. and Combettes, P. (2011). *Convex Analysis and Monotone Operator Theory in Hilbert Spaces*. CMS Books in Mathematics. Springer New York.
- Bhat, S. A. and Huang, N.-F. (2021). Big data and ai revolution in precision agriculture: Survey and challenges. *IEEE Access*, 9:110209–110222.
- Condat, L., Kitahara, D., Contreras, A., and Hirabayashi, A. (2023). Proximal splitting algorithms for convex optimization: A tour of recent advances, with new twists.
- Condat, L. and Richtárik, P. (2023). Randprox: Primal-dual optimization algorithms with randomized proximal updates. In *The Eleventh International Conference on Learning Representations*.
- Esteva, A., Robicquet, A., Ramsundar, B., Kuleshov, V., DePristo, M., Chou, K., Cui, C., Corrado, G., Thrun, S., and Dean, J. (2019). A guide to deep learning in healthcare. *Nature Medicine*, 25(1):24–29.
- Goodell, J. W., Kumar, S., Lim, W. M., and Pattnaik, D. (2021). Artificial intelligence and machine learning in finance: Identifying foundations, themes, and research clusters from bibliometric analysis. *Journal of Behavioral and Experimental Finance*, 32:100577.
- Goodfellow, I., Bengio, Y., and Courville, A. (2016). *Deep Learning*. Adaptive Computation and Machine Learning series. MIT Press.
- Gorbunov, E., Burlachenko, K. P., Li, Z., and Richtárik, P. (2021). Marina: Faster non-convex distributed learning with compression. In Meila, M. and Zhang, T., editors, *Proceedings of the 38th International Conference on Machine Learning*, volume 139 of *Proceedings of Machine Learning Research*, pages 3788–3798. PMLR.
- Gower, R. M., Loizou, N., Qian, X., Sailanbayev, A., Shulgin, E., and Richtárik, P. (2019). SGD: General analysis and improved rates. In *International Conference on Machine Learning*, pages 5200–5209. PMLR.
- Griffiths, D. and Higham, D. (2010). *Numerical Methods for Ordinary Differential Equations: Initial Value Problems*. Springer Undergraduate Mathematics Series. Springer London.
- Grudzień, M., Malinovsky, G., and Richtárik, P. (2023). Can 5th generation local training methods support client sampling? yes! In Ruiz, F., Dy, J., and van de Meent, J.-W., editors, *Proceedings of The 26th International Conference on Artificial Intelligence and Statistics*, volume 206 of *Proceedings of Machine Learning Research*, pages 1055–1092. PMLR.
- Harris, C. R., Millman, K. J., van der Walt, S. J., Gommers, R., Virtanen, P., Cournapeau, D., Wieser, E., Taylor, J., Berg, S., Smith, N. J., Kern, R., Picus, M., Hoyer, S., van Kerkwijk, M. H., Brett, M., Haldane, A., del Río, J. F., Wiebe, M., Peterson, P., Gérard-Marchant, P., Sheppard, K., Reddy, T., Weckesser, W., Abbasi, H., Gohlke, C., and Oliphant, T. E. (2020). Array programming with NumPy. *Nature*, 585(7825):357–362.
- Hofmann, T., Lucchi, A., Lacoste-Julien, S., and McWilliams, B. (2015). Variance reduced stochastic gradient descent with neighbors. In Cortes, C., Lawrence, N., Lee, D., Sugiyama, M., and Garnett, R., editors, *Advances in Neural Information Processing Systems*, volume 28. Curran Associates, Inc.
- Hu, Z. and Huang, H. (2023). Tighter analysis for ProxSkip. In Krause, A., Brunskill, E., Cho, K., Engelhardt, B., Sabato, S., and Scarlett, J., editors, *Proceedings of the 40th International Conference on Machine Learning*, volume 202 of *Proceedings of Machine Learning Research*, pages 13469–13496. PMLR.
- Jhunjunwala, D., Wang, S., and Joshi, G. (2023). Fedexp: Speeding up federated averaging via extrapolation. In *The Eleventh International Conference on Learning Representations*.
- Jiang, X., Rodomanov, A., and Stich, S. U. (2024a). Federated optimization with doubly regularized drift correction. In Salakhutdinov, R., Kolter, Z., Heller, K., Weller, A., Oliver, N., Scarlett, J., and Berkenkamp, F., editors, *Proceedings of the 41st International Conference on Machine Learning*, volume 235 of *Proceedings of Machine Learning Research*, pages 21912–21945. PMLR.
- Jiang, X., Rodomanov, A., and Stich, S. U. (2024b). Stabilized proximal-point methods for federated optimization.
- Johnson, R. and Zhang, T. (2013). Accelerating stochastic gradient descent using predictive variance reduction. In Burges, C., Bottou, L., Welling, M., Ghahramani, Z., and Weinberger, K., editors, *Advances in Neural Information Processing Systems*, volume 26. Curran Associates, Inc.
- Karimireddy, S. P., Kale, S., Mohri, M., Reddi, S., Stich, S., and Suresh, A. T. (2020). SCAFFOLD: Stochastic controlled averaging for federated learning. In III, H. D. and Singh, A., editors, *Proceedings of*

- the 37th International Conference on Machine Learning*, volume 119 of *Proceedings of Machine Learning Research*, pages 5132–5143. PMLR.
- Khaled, A. and Jin, C. (2023). Faster federated optimization under second-order similarity. In *The Eleventh International Conference on Learning Representations*.
- Konečný, J., McMahan, H. B., Yu, F., Richtárik, P., Suresh, A. T., and Bacon, D. (2016). Federated learning: strategies for improving communication efficiency. In *NIPS Private Multi-Party Machine Learning Workshop*.
- Konečný, J. and Richtárik, P. (2015). Semi-stochastic gradient descent methods.
- Kovalev, D., Beznosikov, A., Borodich, E. D., Gasnikov, A., and Scutari, G. (2022). Optimal gradient sliding and its application to optimal distributed optimization under similarity. In Oh, A. H., Agarwal, A., Belgrave, D., and Cho, K., editors, *Advances in Neural Information Processing Systems*.
- Kovalev, D., Horváth, S., and Richtárik, P. (2020). Don't jump through hoops and remove those loops: Svrg and katyusha are better without the outer loop. In Kontorovich, A. and Neu, G., editors, *Proceedings of the 31st International Conference on Algorithmic Learning Theory*, volume 117 of *Proceedings of Machine Learning Research*, pages 451–467. PMLR.
- Li, H., Acharya, K., and Richtárik, P. (2024). The power of extrapolation in federated learning.
- Li, T., Sahu, A. K., Talwalkar, A., and Smith, V. (2020a). Federated learning: Challenges, methods, and future directions. *IEEE Signal Processing Magazine*, 37(3):50–60.
- Li, T., Sahu, A. K., Zaheer, M., Sanjabi, M., Talwalkar, A., and Smith, V. (2020b). Federated optimization in heterogeneous networks.
- Li, Z. (2022). Anita: An optimal loopless accelerated variance-reduced gradient method.
- Li, Z., Bao, H., Zhang, X., and Richtárik, P. (2021). Page: A simple and optimal probabilistic gradient estimator for nonconvex optimization. In Meila, M. and Zhang, T., editors, *Proceedings of the 38th International Conference on Machine Learning*, volume 139 of *Proceedings of Machine Learning Research*, pages 6286–6295. PMLR.
- Li, Z., Kovalev, D., Qian, X., and Richtárik, P. (2020c). Acceleration for compressed gradient descent in distributed and federated optimization. In III, H. D. and Singh, A., editors, *Proceedings of the 37th International Conference on Machine Learning*, volume 119 of *Proceedings of Machine Learning Research*, pages 5895–5904. PMLR.
- Li, Z. and Richtárik, P. (2021). Canita: Faster rates for distributed convex optimization with communication compression. In Ranzato, M., Beygelzimer, A., Dauphin, Y., Liang, P., and Vaughan, J. W., editors, *Advances in Neural Information Processing Systems*, volume 34, pages 13770–13781. Curran Associates, Inc.
- Lin, D., Han, Y., Ye, H., and Zhang, Z. (2023). Stochastic distributed optimization under average second-order similarity: Algorithms and analysis. In Oh, A., Naumann, T., Globerson, A., Saenko, K., Hardt, M., and Levine, S., editors, *Advances in Neural Information Processing Systems*, volume 36, pages 1849–1862. Curran Associates, Inc.
- Maleki Varnosfaderani, S. and Forouzanfar, M. (2024). The role of ai in hospitals and clinics: transforming healthcare in the 21st century. *Bioengineering*, 11(4):337.
- Malinovsky, G., Yi, K., and Richtárik, P. (2022). Variance reduced proxskip: Algorithm, theory and application to federated learning. In Oh, A. H., Agarwal, A., Belgrave, D., and Cho, K., editors, *Advances in Neural Information Processing Systems*.
- McMahan, H. B., Moore, E., Ramage, D., Hampson, S., and y Arcas, B. A. (2017). Communication-efficient learning of deep networks from decentralized data. In *Proceedings of the 20th International Conference on Artificial Intelligence and Statistics (AISTATS)*.
- Mishchenko, K., Li, R., Fan, H., and Venieris, S. (2024). Federated learning under second-order data heterogeneity.
- Mishchenko, K., Malinovsky, G., Stich, S., and Richtárik, P. (2022). ProxSkip: Yes! Local gradient steps provably lead to communication acceleration! Finally! In Chaudhuri, K., Jegelka, S., Song, L., Szepesvari, C., Niu, G., and Sabato, S., editors, *Proceedings of the 39th International Conference on Machine Learning*, volume 162 of *Proceedings of Machine Learning Research*, pages 15750–15769. PMLR.
- Nesterov, Y. et al. (2018). *Lectures on convex optimization*, volume 137. Springer.
- Nguyen, L. M., Liu, J., Scheinberg, K., and Takáč, M. (2017). SARAH: A novel method for machine learning problems using stochastic recursive gradient. In Precup, D. and Teh, Y. W., editors, *Proceedings of the 34th International Conference on Machine Learning*, volume 70 of *Proceedings of Machine Learning Research*, pages 2613–2621. PMLR.
- Oosthuizen, K., Botha, E., Robertson, J., and Montecchi, M. (2021). Artificial intelligence in retail: The ai-enabled value chain. *Australasian Marketing Journal*, 29(3):264–273.

- Parikh, N. and Boyd, S. (2013). *Proximal Algorithms*. Foundations and Trends® in Optimization Series. Now Publishers.
- Richtárik, P., Sadiev, A., and Demidovich, Y. (2024a). A unified theory of stochastic proximal point methods without smoothness.
- Richtárik, P., Sadiev, A., and Demidovich, Y. (2024b). A unified theory of stochastic proximal point methods without smoothness.
- Robbins, H. and Monro, S. (1951). A stochastic approximation method. *The annals of mathematical statistics*, pages 400–407.
- Ryu, E. and Boyd, S. (2016). Stochastic proximal iteration: A non-asymptotic improvement upon stochastic gradient descent. Technical report, Stanford University.
- Sadiev, A., Condat, L., and Richtárik, P. (2024). Stochastic proximal point methods for monotone inclusions under expected similarity.
- Sebbouh, O., Cuturi, M., and Peyré, G. (2022). Randomized stochastic gradient descent ascent. In Camps-Valls, G., Ruiz, F. J. R., and Valera, I., editors, *Proceedings of The 25th International Conference on Artificial Intelligence and Statistics*, volume 151 of *Proceedings of Machine Learning Research*, pages 2941–2969. PMLR.
- Shalev-Shwartz, S. and Ben-David, S. (2014). *Understanding machine learning: From theory to algorithms*. Cambridge university press.
- Shamir, O., Srebro, N., and Zhang, T. (2014). Communication-efficient distributed optimization using an approximate newton-type method. In Xing, E. P. and Jebara, T., editors, *Proceedings of the 31st International Conference on Machine Learning*, volume 32 of *Proceedings of Machine Learning Research*, pages 1000–1008, Beijing, China. PMLR.
- Sun, Y., Daneshmand, A., and Scutari, G. (2020). Distributed optimization based on gradient-tracking revisited: Enhancing convergence rate via surrogation.
- Szlendak, R., Tyurin, A., and Richtárik, P. (2022). Permutation compressors for provably faster distributed nonconvex optimization. In *International Conference on Learning Representations*.
- T. Dinh, C., Tran, N., and Nguyen, J. (2020). Personalized federated learning with moreau envelopes. In Larochelle, H., Ranzato, M., Hadsell, R., Balcan, M., and Lin, H., editors, *Advances in Neural Information Processing Systems*, volume 33, pages 21394–21405. Curran Associates, Inc.
- Traoré, C., Apidopoulos, V., Salzo, S., and Villa, S. (2024). Variance reduction techniques for stochastic proximal point algorithms. *Journal of Optimization Theory and Applications*, 203(2):1910–1939.
- Virtanen, P., Gommers, R., Oliphant, T. E., Haberland, M., Reddy, T., Cournapeau, D., Burovski, E., Peterson, P., Weckesser, W., Bright, J., van der Walt, S. J., Brett, M., Wilson, J., Millman, K. J., Mayorov, N., Nelson, A. R. J., Jones, E., Kern, R., Larson, E., Carey, C. J., Polat, İ., Feng, Y., Moore, E. W., VanderPlas, J., Laxalde, D., Perktold, J., Cimrman, R., Henriksen, I., Quintero, E. A., Harris, C. R., Archibald, A. M., Ribeiro, A. H., Pedregosa, F., van Mulbregt, P., and SciPy 1.0 Contributors (2020). SciPy 1.0: Fundamental Algorithms for Scientific Computing in Python. *Nature Methods*, 17:261–272.
- Wen, Y., Fashiar Rahman, M., Xu, H., and Tseng, T.-L. B. (2022). Recent advances and trends of predictive maintenance from data-driven machine prognostics perspective. *Measurement*, 187:110276.
- Woodworth, B., Mishchenko, K., and Bach, F. (2023). Two losses are better than one: Faster optimization using a cheaper proxy. In Krause, A., Brunskill, E., Cho, K., Engelhardt, B., Sabato, S., and Scarlett, J., editors, *Proceedings of the 40th International Conference on Machine Learning*, volume 202 of *Proceedings of Machine Learning Research*, pages 37273–37292. PMLR.
- Woodworth, B. E. and Srebro, N. (2016). Tight complexity bounds for optimizing composite objectives. In Lee, D., Sugiyama, M., Luxburg, U., Guyon, I., and Garnett, R., editors, *Advances in Neural Information Processing Systems*, volume 29. Curran Associates, Inc.
- Yan, Y., Xu, Y., Lin, Q., Liu, W., and Yang, T. (2020). Optimal epoch stochastic gradient descent ascent methods for min-max optimization. In Larochelle, H., Ranzato, M., Hadsell, R., Balcan, M., and Lin, H., editors, *Advances in Neural Information Processing Systems*, volume 33, pages 5789–5800. Curran Associates, Inc.
- Zhang, J., He, T., Sra, S., and Jadbabaie, A. (2020). Why gradient clipping accelerates training: A theoretical justification for adaptivity. In *International Conference on Learning Representations*.

Checklist

1. For all models and algorithms presented, check if you include:
 - (a) A clear description of the mathematical setting, assumptions, algorithm, and/or model. Yes
 - (b) An analysis of the properties and complexity (time, space, sample size) of any algorithm. Yes
 - (c) (Optional) Anonymized source code, with specification of all dependencies, including external libraries.
2. For any theoretical claim, check if you include:
 - (a) Statements of the full set of assumptions of all theoretical results. Yes
 - (b) Complete proofs of all theoretical results. Yes
 - (c) Clear explanations of any assumptions. Yes
3. For all figures and tables that present empirical results, check if you include:
 - (a) The code, data, and instructions needed to reproduce the main experimental results (either in the supplemental material or as a URL). Yes
 - (b) All the training details (e.g., data splits, hyperparameters, how they were chosen). Yes
 - (c) A clear definition of the specific measure or statistics and error bars (e.g., with respect to the random seed after running experiments multiple times). Yes
 - (d) A description of the computing infrastructure used. (e.g., type of GPUs, internal cluster, or cloud provider). Yes
4. If you are using existing assets (e.g., code, data, models) or curating/releasing new assets, check if you include:
 - (a) Citations of the creator If your work uses existing assets. Yes
 - (b) The license information of the assets, if applicable. Not Applicable
 - (c) New assets either in the supplemental material or as a URL, if applicable. Not Applicable
 - (d) Information about consent from data providers/curators. Not Applicable
 - (e) Discussion of sensible content if applicable, e.g., personally identifiable information or offensive content. Not Applicable
5. If you used crowdsourcing or conducted research with human subjects, check if you include:
 - (a) The full text of instructions given to participants and screenshots. Not Applicable
 - (b) Descriptions of potential participant risks, with links to Institutional Review Board (IRB) approvals if applicable. Not Applicable
 - (c) The estimated hourly wage paid to participants and the total amount spent on participant compensation. Not Applicable

A Auxiliary facts

For ease of reference, we present the following standard lemmas.

Lemma 3. Let $\{a_i\}_{i=1}^n$ be a set of arbitrary vectors in \mathbb{R}^d . Let the average vector be denoted as $\bar{a} = \frac{1}{n} \sum_{i=1}^n a_i$. Then, the following identity holds:

$$\frac{1}{n} \sum_{i=1}^n \|a_i - \bar{a}\|^2 = \frac{1}{n} \sum_{i=1}^n \|a_i\|^2 - \|\bar{a}\|^2. \quad (26)$$

Proof. The proof is straight-forward.

$$\begin{aligned} \frac{1}{n} \sum_{i=1}^n \|a_i - \bar{a}\|^2 &= \frac{1}{n} \sum_{i=1}^n [\|a_i\|^2 + \|\bar{a}\|^2 - 2\langle a_i, \bar{a} \rangle] \\ &= \frac{1}{n} \sum_{i=1}^n \|a_i\|^2 + \|\bar{a}\|^2 - 2\frac{1}{n} \sum_{i=1}^n \langle a_i, \bar{a} \rangle \\ &= \frac{1}{n} \sum_{i=1}^n \|a_i\|^2 + \|\bar{a}\|^2 - 2\left\langle \frac{1}{n} \sum_{i=1}^n a_i, \bar{a} \right\rangle \\ &= \frac{1}{n} \sum_{i=1}^n \|a_i\|^2 + \|\bar{a}\|^2 - 2\|\bar{a}\|^2 \\ &= \frac{1}{n} \sum_{i=1}^n \|a_i\|^2 - \|\bar{a}\|^2. \end{aligned}$$

□

Lemma 4. For any vectors $a, b \in \mathbb{R}^d$ and a positive scalar $\zeta > 0$, it holds that

$$\langle a, b \rangle - \frac{1}{2\zeta} \|a\|^2 \leq \frac{\zeta}{2} \|b\|^2. \quad (27)$$

Proof. Expanding the quadratics, we get:

$$0 \leq \frac{1}{2} \left\| \sqrt{\zeta} b - \frac{1}{\sqrt{\zeta}} a \right\|^2 = \frac{1}{2} \left[\zeta \|b\|^2 + \frac{1}{\zeta} \|a\|^2 - 2\langle a, b \rangle \right].$$

It remains to rearrange the terms to finish the proof. □

We also present key properties of proximity operators.

Definition 4. Let $f : \mathbb{R}^d \rightarrow \mathbb{R} \cup \{+\infty\}$ be a proper, closed, convex function and $\gamma > 0$ be a positive scalar. Then, the proximal operator with respect to f is defined as follows:

$$\text{prox}_{\gamma f}(x) = \underset{y \in \mathbb{R}^d}{\text{argmin}} \left\{ \frac{1}{2\gamma} \|x - y\|^2 + f(y) \right\}. \quad (28)$$

Lemma 5 (Proposition 16.44, (Bauschke and Combettes, 2011)). Let $f : \mathbb{R}^d \rightarrow \mathbb{R} \cup \{+\infty\}$ be a proper, closed, convex function and $\gamma > 0$ be a positive scalar. Then,

$$\text{prox}_{\gamma f}(x) = y \Leftrightarrow x - y \in \gamma \partial f(y). \quad (29)$$

Lemma 6. Let $f : \mathbb{R}^d \rightarrow \mathbb{R}$ be a μ -strongly convex function (Assumption 2). Then, for any $x, y \in \mathbb{R}^d$ and any $\gamma > 0$, the proximity operator satisfies

$$\|\text{prox}_{\gamma f}(x) - \text{prox}_{\gamma f}(y)\|^2 \leq \frac{1}{(1 + \gamma\mu)^2} \|x - y\|^2. \quad (30)$$

Proof. Let us denote $x' = \text{prox}_{\gamma f}(x)$ and $y' = \text{prox}_{\gamma f}(y)$. By the optimality condition of the proximal operator, we have

$$x - x' = \gamma \nabla f(x'), \quad y - y' = \gamma \nabla f(y').$$

Subtracting these two equations yields

$$x - y = x' - y' + \gamma(\nabla f(x') - \nabla f(y')).$$

Taking the inner product with $x' - y'$, we obtain

$$\langle x - y, x' - y' \rangle = \|x' - y'\|^2 + \gamma \langle \nabla f(x') - \nabla f(y'), x' - y' \rangle.$$

Using the strong convexity of f , we have

$$\langle \nabla f(x') - \nabla f(y'), x' - y' \rangle \geq \mu \|x' - y'\|^2. \quad (31)$$

Substituting inequality (31) into the previous expression, we get

$$\langle x - y, x' - y' \rangle \geq (1 + \gamma\mu) \|x' - y'\|^2.$$

By the Cauchy–Schwarz inequality,

$$\|x - y\| \|x' - y'\| \geq \langle x - y, x' - y' \rangle.$$

Combining the two inequalities, we obtain

$$\|x - y\| \|x' - y'\| \geq (1 + \gamma\mu) \|x' - y'\|^2,$$

which simplifies to

$$\|x' - y'\| \leq \frac{1}{1 + \gamma\mu} \|x - y\|.$$

This completes the proof. □

B Proof of Lemma 1

We begin by introducing the following technical lemma, which follows the proof strategy of the **DANE** algorithm as described in (Jiang et al., 2024a).

Lemma 7. *Let Assumption 2 (strong convexity) hold. Let us define*

$$\bar{x}_{k+1} \stackrel{\text{def}}{=} \mathbb{E}[x_{k+1} | x_k, w_k] \quad (32)$$

and

$$\psi_i(x) \stackrel{\text{def}}{=} f_i(x) - f(x). \quad (33)$$

Then, after one iteration of Algorithm 3, for any $y \in \mathbb{R}^d$, the following inequality holds:

$$\begin{aligned} \mathbb{E}[\|x_{k+1} - x_*\|^2 | x_k, w_k] &\leq \frac{1}{1 + \mu\gamma} \|x_k - x_*\|^2 && \text{(contraction)} \\ &\quad - \frac{2}{\mu + \frac{1}{\gamma}} [f(y) - f(x_*)] && \text{(always } \leq 0) \\ - \frac{2}{\mu + \frac{1}{\gamma}} \mathbb{E} \left[\langle \nabla \psi_{i_k}(y) - \nabla \psi_{i_k}(w_k), x_{k+1} - y \rangle + \frac{\mu + \frac{1}{\gamma}}{2} \|x_{k+1} - y\|^2 | x_k, w_k \right] &&& \text{(bounded by } \leq \frac{\delta^2 \|y - w_k\|^2}{(\mu + \frac{1}{\gamma})^2}) \\ &\quad - \frac{1}{1 + \mu\gamma} \|y - x_k\|^2 && \text{(negative term)} \\ - \frac{2}{1 + \mu\gamma} \langle \bar{x}_{k+1} - y, y + \gamma \nabla f(y) - x_k \rangle &&& \text{(remaining term)} \end{aligned} .$$

Remark 5. To eliminate the "remaining" term, represented by the scalar product, it is necessary to choose $y \in \mathbb{R}^d$ such that $\langle \bar{x}_{k+1} - y, y + \gamma \nabla f(y) - x_k \rangle \geq 0$. This condition is satisfied, for example, when $y = \text{prox}_{\gamma f}(x_k)$ or $y = \bar{x}_{k+1}$.

Proof. In this proof, all expectations are taken with respect to x_k and w_k . Let us denote $h_k = \nabla f_{i_k}(w_k) - \nabla f(w_k)$. We begin as follows:

$$\begin{aligned}
 x_{k+1} &\stackrel{\text{Alg. 3}}{=} \text{prox}_{\gamma f_{i_k}}(x_k + \gamma h_k) \\
 &\stackrel{(28)}{=} \underset{x \in \mathbb{R}^d}{\text{argmin}} \left\{ f_{\xi_k}(x) + \frac{1}{2\gamma} \|x - x_k - \gamma h_k\|^2 \right\} \\
 &= \underset{x \in \mathbb{R}^d}{\text{argmin}} \left\{ f_{\xi_k}(x) + \frac{1}{2\gamma} [\|x - x_k\|^2 + \gamma^2 \|h_k\|^2 - 2\gamma \langle x - x_k, h_k \rangle] \right\} \\
 &= \underset{x \in \mathbb{R}^d}{\text{argmin}} \left\{ f_{\xi_k}(x) + \frac{1}{2\gamma} \|x - x_k\|^2 - \langle x, h_k \rangle + \frac{\gamma}{2} \|h_k\|^2 + \langle x_k, h_k \rangle \right\} \\
 &= \underset{x \in \mathbb{R}^d}{\text{argmin}} \left\{ f_{\xi_k}(x) - \langle x, h_k \rangle + \frac{1}{2\gamma} \|x - x_k\|^2 \right\}.
 \end{aligned} \tag{34}$$

For brevity, we denote $f_{i_k}^k(x) \stackrel{\text{def}}{=} f_{i_k}(x) - \langle x, \nabla f_{i_k}(w_k) - \nabla f(w_k) \rangle + \frac{1}{2\gamma} \|x - x_k\|^2$. Then, according to (34),

$$x_{k+1} = \underset{x \in \mathbb{R}^d}{\text{argmin}} f_{i_k}^k(x). \tag{35}$$

By leveraging the $\mu + \frac{1}{\gamma}$ -strong convexity of $f_{i_k}^k$ and applying (35), we derive the following for any $x \in \mathbb{R}^d$:

$$f_{i_k}^k(x) \geq f_{i_k}^k(x_{k+1}) + \frac{\mu + \frac{1}{\gamma}}{2} \|x - x_{k+1}\|^2.$$

Expanding $f_{i_k}^k$, we obtain

$$\begin{aligned}
 &f_{i_k}(x) - \langle x, \nabla f_{i_k}(w_k) - \nabla f(w_k) \rangle + \frac{1}{2\gamma} \|x - x_k\|^2 \\
 &\geq f_{i_k}(x_{k+1}) - \langle x_{k+1}, \nabla f_{i_k}(w_k) - \nabla f(w_k) \rangle + \frac{1}{2\gamma} \|x_{k+1} - x_k\|^2 + \frac{\mu + \frac{1}{\gamma}}{2} \|x - x_{k+1}\|^2.
 \end{aligned}$$

Exploiting the strong convexity of f_{i_k} , we further obtain the following for any arbitrary $y \in \mathbb{R}^d$:

$$\begin{aligned}
 &f_{i_k}(x) - \langle x, \nabla f_{i_k}(w_k) - \nabla f(w_k) \rangle + \frac{1}{2\gamma} \|x - x_k\|^2 \\
 &\geq f_{i_k}(y) + \langle \nabla f_{i_k}(y), x_{k+1} - y \rangle + \frac{\mu}{2} \|y - x_{k+1}\|^2 \\
 &\quad - \langle x_{k+1}, \nabla f_{i_k}(w_k) - \nabla f(w_k) \rangle + \frac{1}{2\gamma} \|x_{k+1} - x_k\|^2 + \frac{\mu + \frac{1}{\gamma}}{2} \|x - x_{k+1}\|^2.
 \end{aligned}$$

By taking the conditional expectation $\mathbb{E}[\cdot | x_k, w_k]$, we get

$$\begin{aligned}
 f(x) + \frac{1}{2\gamma} \|x - x_k\|^2 &\geq f(y) + \frac{\mu + \frac{1}{\gamma}}{2} \mathbb{E}[\|x - x_{k+1}\|^2] \\
 &\quad + \mathbb{E}[\langle \nabla f_{i_k}(y), x_{k+1} - y \rangle - \langle x_{k+1}, \nabla f_{i_k}(w_k) - \nabla f(w_k) \rangle] + \mathbb{E}\left[\frac{\mu}{2} \|x_{k+1} - y\|^2 + \frac{1}{2\gamma} \|x_{k+1} - x_k\|^2\right].
 \end{aligned} \tag{36}$$

Recall that $\psi_{i_k} \stackrel{\text{def}}{=} f_{i_k} - f$. Given that $\mathbb{E}[\langle y, \nabla f_{i_k}(w_k) - \nabla f(w_k) \rangle | x_k, w_k] = 0$, we additionally observe

$$\begin{aligned}
 &\mathbb{E}[\langle \nabla f_{i_k}(y), x_{k+1} - y \rangle - \langle x_{k+1}, \nabla f_{i_k}(w_k) - \nabla f(w_k) \rangle] \\
 &= \mathbb{E}[\langle \nabla f_{i_k}(y) - \nabla f(y) - [\nabla f_{i_k}(w_k) - \nabla f(w_k)], x_{k+1} - y \rangle] + \mathbb{E}[\langle \nabla f(y), x_{k+1} - y \rangle] \\
 &= \mathbb{E}[\langle \nabla f_{i_k}(y) - \nabla f(y) - [\nabla f_{i_k}(w_k) - \nabla f(w_k)], x_{k+1} - y \rangle] + \langle \nabla f(y), \bar{x}_{k+1} - y \rangle \\
 &= \mathbb{E}[\langle \nabla \psi_{i_k}(y) - \nabla \psi_{i_k}(w_k), x_{k+1} - y \rangle] + \langle \nabla f(y), \bar{x}_{k+1} - y \rangle.
 \end{aligned}$$

It is also evident that

$$\begin{aligned}
 & \mathbb{E} \left[\frac{\mu}{2} \|x_{k+1} - y\|^2 + \frac{1}{2\gamma} \|x_{k+1} - x_k\|^2 \right] \\
 &= \mathbb{E} \left[\frac{\mu}{2} \|x_{k+1} - y\|^2 + \frac{1}{2\gamma} \|x_{k+1} - y\|^2 + \frac{1}{2\gamma} \|y - x_k\|^2 + \frac{1}{\gamma} \langle x_{k+1} - y, y - x_k \rangle \right] \\
 &= \mathbb{E} \left[\frac{\mu + \frac{1}{\gamma}}{2} \|x_{k+1} - y\|^2 \right] + \frac{1}{2\gamma} \|y - x_k\|^2 + \frac{1}{\gamma} \langle \bar{x}_{k+1} - y, y - x_k \rangle.
 \end{aligned}$$

Plugging last two equations into (36), we obtain

$$\begin{aligned}
 f(x) + \frac{1}{2\gamma} \|x - x_k\|^2 &\geq f(y) + \frac{\mu + \frac{1}{\gamma}}{2} \mathbb{E} [\|x - x_{k+1}\|^2] \\
 &+ \mathbb{E} [\langle \nabla \psi_{i_k}(y) - \nabla \psi_{i_k}(w_k), x_{k+1} - y \rangle] + \langle \nabla f(y), \bar{x}_{k+1} - y \rangle \\
 &+ \mathbb{E} \left[\frac{\mu + \frac{1}{\gamma}}{2} \|x_{k+1} - y\|^2 \right] + \frac{1}{2\gamma} \|y - x_k\|^2 + \frac{1}{\gamma} \langle \bar{x}_{k+1} - y, y - x_k \rangle.
 \end{aligned}$$

Rearranging terms, we get

$$\begin{aligned}
 f(x) + \frac{1}{2\gamma} \|x - x_k\|^2 &\geq f(y) + \frac{\mu + \frac{1}{\gamma}}{2} \mathbb{E} [\|x - x_{k+1}\|^2] + \frac{1}{\gamma} \langle \bar{x}_{k+1} - y, y + \gamma \nabla f(y) - x_k \rangle \\
 &+ \mathbb{E} [\langle \nabla \psi_{i_k}(y) - \nabla \psi_{i_k}(w_k), x_{k+1} - y \rangle] + \frac{\mu + \frac{1}{\gamma}}{2} \mathbb{E} [\|x_{k+1} - y\|^2] + \frac{1}{2\gamma} \|y - x_k\|^2.
 \end{aligned}$$

Rearranging the terms once again and setting $x = x_*$, we have:

$$\begin{aligned}
 \mathbb{E} [\|x_{k+1} - x_*\|^2] &\leq \frac{1}{1 + \mu\gamma} \|x_k - x_*\|^2 && \text{(contraction)} \\
 &\quad - \frac{2}{\mu + \frac{1}{\gamma}} [f(y) - f(x_*)] && \text{(always } \leq 0) \\
 - \frac{2}{\mu + \frac{1}{\gamma}} \mathbb{E} \left[\langle \nabla \psi_{i_k}(y) - \nabla \psi_{i_k}(w_k), x_{k+1} - y \rangle + \frac{\mu + \frac{1}{\gamma}}{2} \|x_{k+1} - y\|^2 \right] &&& \text{(can be bounded by } \leq \frac{\delta^2 \|y - w_k\|^2}{(\mu + \frac{1}{\gamma})^2}) \\
 - \frac{1}{1 + \mu\gamma} \|y - x_k\|^2 - \frac{2}{1 + \mu\gamma} \langle \bar{x}_{k+1} - y, y + \gamma \nabla f(y) - x_k \rangle &&& \text{(remaining terms)} \quad .
 \end{aligned}$$

□

The proof of Lemma 1 now follows as a corollary of Lemma 7.

Proof of Lemma 1. If we substitute $y = \bar{x}_{k+1}$ into Lemma 7, the last term, $\langle \bar{x}_{k+1} - y, y + \gamma \nabla f(y) - x_k \rangle|_{y=\bar{x}_{k+1}} = 0$. Furthermore, by noting that $f(\bar{x}_{k+1}) - f(x_*) \geq 0$, the statement can be established with the application of Lemma 7.

C Proof of Theorem 1

Proof. Recall that the Lyapunov sequence is defined as follows:

$$\Lambda_k = \|x_k - x_*\|^2 + c\|w_k - x_k\|^2. \tag{37}$$

Combining Lemma 1 and Lemma 2, we obtain:

$$\begin{aligned}
 \mathbb{E} [\Lambda_{k+1} | x_k, w_k] &\stackrel{(37)}{=} \mathbb{E} [\|x_{k+1} - x_*\|^2 | x_k, w_k] + c\mathbb{E} [\|w_{k+1} - x_{k+1}\|^2 | x_k, w_k] \\
 &\stackrel{(9)+(10)}{\leq} \frac{1}{1 + \mu\gamma} \|x_k - x_*\|^2
 \end{aligned}$$

$$\begin{aligned}
 & -\frac{2}{\mu + \frac{1}{\gamma}} \mathbb{E} \left[\langle \nabla \psi_{i_k}(\bar{x}_{k+1}) - \nabla \psi_{i_k}(w_k), x_{k+1} - \bar{x}_{k+1} \rangle + \frac{\mu + \frac{1}{\gamma}}{2} \|x_{k+1} - \bar{x}_{k+1}\|^2 \right] \\
 & -\frac{1}{1 + \mu\gamma} \|\bar{x}_{k+1} - x_k\|^2 \\
 & + (1 - p(1 - \xi))(1 + \zeta)c \|w_k - x_k\|^2 \\
 & + (1 - p(1 - \xi))(1 + \zeta^{-1})c \|x_k - \bar{x}_{k+1}\|^2 \\
 & - cp\xi \|w_k - \bar{x}_{k+1}\|^2 \\
 & + c(1 - p) \mathbb{E} [\|\bar{x}_{k+1} - x_{k+1}\|^2 | x_k, w_k] \\
 = & \frac{1}{1 + \mu\gamma} \|x_k - x_*\|^2 + (1 - p(1 - \xi))(1 + \zeta)c \|w_k - x_k\|^2 \tag{38} \\
 & -\frac{2}{\mu + \frac{1}{\gamma}} \mathbb{E} \left[\langle \nabla \psi_{i_k}(\bar{x}_{k+1}) - \nabla \psi_{i_k}(w_k), x_{k+1} - \bar{x}_{k+1} \rangle + \frac{\mu + \frac{1}{\gamma}}{2} (1 - c(1 - p)) \|x_{k+1} - \bar{x}_{k+1}\|^2 \right] \\
 & -cp\xi \|w_k - \bar{x}_{k+1}\|^2 \\
 & + \|\bar{x}_{k+1} - x_k\|^2 \left[(1 - p(1 - \xi))(1 + \zeta^{-1})c - \frac{1}{1 + \mu\gamma} \right] \\
 \stackrel{(27)}{\leq} & \max \left\{ \frac{1}{1 + \mu\gamma}, 1 - p(1 - \xi)(1 + \zeta) \right\} \Lambda_k \\
 & + \frac{2}{\mu + \frac{1}{\gamma}} \frac{1}{2 \left(\mu + \frac{1}{\gamma} \right) (1 - c(1 - p))} \mathbb{E} [\|\nabla \psi_{i_k}(\bar{x}_{k+1}) - \nabla \psi_{i_k}(w_k)\|^2] \\
 & -cp\xi \|w_k - \bar{x}_{k+1}\|^2,
 \end{aligned}$$

where we drop the last term since we enforce $c \leq \frac{1}{(1 + \mu\gamma)(1 - p(1 - \xi))(1 + \zeta^{-1})}$. Additionally, observe that

$$c \leq \frac{1}{(1 + \mu\gamma)(1 - p(1 - \xi))(1 + \zeta^{-1})} < \frac{1}{1 - p(1 - \xi)} < \frac{1}{1 - p}.$$

Therefore, $(1 - c(1 - p)) \frac{\mu + \frac{1}{\gamma}}{2} > 0$, and Lemma 4 is applicable. Then, we continue

$$\begin{aligned}
 \mathbb{E} [\Lambda_{k+1} | x_k, w_k] & \stackrel{(38)}{\leq} \max \left\{ \frac{1}{1 + \mu\gamma}, (1 - p(1 - \xi))(1 + \zeta) \right\} \Lambda_k \\
 & + \frac{2}{\mu + \frac{1}{\gamma}} \frac{1}{2 \left(\mu + \frac{1}{\gamma} \right) (1 - c(1 - p))} \mathbb{E} [\|\nabla \psi_{i_k}(\bar{x}_{k+1}) - \nabla \psi_{i_k}(w_k)\|^2] \\
 & -cp\xi \|w_k - \bar{x}_{k+1}\|^2 \\
 & \stackrel{(2)}{\leq} \max \left\{ \frac{1}{1 + \mu\gamma}, (1 - p(1 - \xi))(1 + \zeta) \right\} \Lambda_k \\
 & + \frac{1}{\left(\mu + \frac{1}{\gamma} \right)^2 (1 - c(1 - p))} \delta^2 \|w_k - \bar{x}_{k+1}\|^2 \\
 & -cp\xi \|w_k - \bar{x}_{k+1}\|^2 \\
 & \leq \max \left\{ \frac{1}{1 + \mu\gamma}, (1 - p(1 - \xi))(1 + \zeta) \right\} \Lambda_k,
 \end{aligned}$$

since we enforce $\frac{\delta^2}{\left(\mu + \frac{1}{\gamma} \right)^2 (1 - c(1 - p))} \leq cp\xi$. To complete the proof, it remains to take the full expectation of both sides. \square

D Proof of Corollary 3

Proof. Let us define

$$a \stackrel{\text{def}}{=} \frac{2(3 - p)^2}{p^2(p + 1)}. \tag{39}$$

According to Corollary 1, the stepsize γ must satisfy the inequality

$$a\delta^2\gamma^2 - \mu\gamma - 1 \leq 0.$$

We verify that the choice $\gamma' = \frac{1}{\delta\sqrt{a}}$ satisfies this condition: $a\delta^2\gamma'^2 - \mu\gamma' - 1 = -\mu\gamma' \leq 0$. By (18), we have

$$\mathbb{E} [\|x_T - x_*\|^2] \leq \max \left\{ 1 - \frac{\mu\gamma'}{1 + \mu\gamma'}, 1 - \frac{p}{4} \right\}^T \|x_0 - x_*\|^2.$$

To achieve $\mathbb{E} [\|x_T - x_*\|^2] \leq \varepsilon$, we need to satisfy

$$\begin{aligned} T &\geq \left(1 + \frac{1}{\mu\gamma'} + \frac{4}{p} \right) \log \left(\frac{\|x_0 - x_*\|^2}{\varepsilon} \right) \\ &= \left(1 + \frac{\delta\sqrt{a}}{\mu} + \frac{4}{p} \right) \log \left(\frac{\|x_0 - x_*\|^2}{\varepsilon} \right) \\ &\stackrel{(39)}{=} \left(1 + \frac{\delta}{\mu} \frac{3-p}{p} \sqrt{\frac{2}{p+1}} + \frac{4}{p} \right) \log \left(\frac{\|x_0 - x_*\|^2}{\varepsilon} \right) \Leftarrow \\ T &\geq \left(1 + \frac{\delta}{\mu} \frac{3}{p} + \frac{4}{p} \right) \log \left(\frac{\|x_0 - x_*\|^2}{\varepsilon} \right), \end{aligned}$$

what completes the proof. □

E Convex analysis

The result established for strongly convex functions can be seamlessly extended to the convex case. In summary, all findings presented in the earlier sections remain valid when $\mu = 0$ and for any $x_* \in \text{Argmin } f$ (noting that if $\mu > 0$, the minimizer is unique). However, a key challenge arises: the primary result for strongly convex functions does not yield contraction when $\mu = 0$. Nevertheless, by employing a few modifications to the existing proof, it is possible to derive a new convergence rate.

Lemma 8. *Let Assumption 2 (strong convexity) hold. Let us define $\psi_i(x) \stackrel{\text{def}}{=} f_i(x) - f(x)$, and $x_* \in \text{Argmin } f$, and $f^* = \min_{x \in \mathbb{R}^d} f(x)$. Then, for one iteration of Algorithm 3, the following inequality holds:*

$$\begin{aligned} \mathbb{E} [\|x_{k+1} - x_*\|^2 | x_k, w_k] &\leq \frac{1}{1 + \mu\gamma} \|x_k - x_*\|^2 - \frac{2}{\mu + \frac{1}{\gamma}} (f(\bar{x}_{k+1}) - f^*) - \mathbb{E} [\|x_{k+1} - \bar{x}_{k+1}\|^2] \\ &\quad - \frac{1}{1 + \mu\gamma} \|\bar{x}_{k+1} - x_k\|^2 - \frac{2}{\mu + \frac{1}{\gamma}} \mathbb{E} [\langle \nabla \psi_{i_k}(\bar{x}_{k+1}) - \nabla \psi_{i_k}(w_k), x_{k+1} - \bar{x}_{k+1} \rangle | x_k, w_k]. \end{aligned} \quad (40)$$

Proof. Recall that the proof of Lemma 1 relies on the technical Lemma 7 by assigning a specific value to y and, more importantly, explicitly eliminating the negative term $-\frac{2}{\mu + \frac{1}{\gamma}} f(\bar{x}_{k+1}) - f^*$. If we retain the functional difference term, we obtain the proof of the current lemma. \square

Preserving Lemma 2 unchanged, we will reformulate the result of Theorem 1 by utilizing Lemma 8 in place of Lemma 1, while following the exact same sequence of derivations. This approach yields Theorem 6.

Theorem 6. *Let Assumptions 1 and 2 hold. Let $x_* \in \text{Argmin } f$ and $f^* = \min_{x \in \mathbb{R}^d} f(x)$. For a given $\xi \in [0, 1]$ and constants $c > 0$, $\gamma > 0$, and $\zeta > 0$, suppose the following inequalities are satisfied:*

$$c \leq \frac{1}{(1 + \mu\gamma)(1 - p(1 - \xi))(1 + \zeta^{-1})}, \quad (41)$$

$$cp\xi \geq \frac{\delta^2}{\left(\mu + \frac{1}{\gamma}\right)^2 (1 - c(1 - p))}, \quad (42)$$

$$1 - r = (1 - p(1 - \xi))(1 + \zeta) \quad (43)$$

where r is a positive constant, and $p \in (0, 1]$ is the probability parameter from Algorithm 3.

Define the Lyapunov function:

$$\Lambda_k \stackrel{\text{def}}{=} \|x_k - x_*\|^2 + c\|w_k - x_k\|^2.$$

where x_k and w_k are the iterates of Algorithm 3, and x_* is the unique solution to problem (1). Then, the iterates satisfy:

$$\mathbb{E} [\Lambda_{k+1}] \leq \max \left\{ \frac{1}{1 + \mu\gamma}, 1 - r \right\} \mathbb{E} [\Lambda_k] - \frac{2}{\mu + \frac{1}{\gamma}} (\mathbb{E} [f(\bar{x}_{k+1})] - f^*), \quad (44)$$

Proof. The proof follows the same sequence of derivations as in the proof of Theorem 1, with the sole difference being that Lemma 8 is applied instead of Lemma 1. \square

We are now ready to establish the result for convex functions.

Proof of Corollary 2

Proof. As shown in the proof of Corollary 1, equations (19) and (17) ensure that the following conditions satisfy inequalities (41), (42), and (43):

$$c = \frac{2p}{(3 - p)^2} \frac{1}{1 + \mu\gamma}, \quad \xi = \frac{1}{2}, \quad r = \frac{p}{4},$$

and we replicate the condition on γ into (22).

By rearranging the terms in (44), we obtain

$$\frac{2}{\mu + \frac{1}{\gamma}} [\mathbb{E} [f(\bar{x}_{k+1})] - f^*] \stackrel{(44)}{\leq} \left[\max \left\{ \frac{1}{1 + \mu\gamma}, 1 - r \right\} \mathbb{E} [\Lambda_k] - \mathbb{E} [\Lambda_{k+1}] \right] \leq \mathbb{E} [\Lambda_k] - \mathbb{E} [\Lambda_{k+1}]. \quad (45)$$

To complete the proof, we sum all inequalities of this form over $k = 0, \dots, K - 1$ and rearrange the terms as follows:

$$\frac{2}{\mu + \frac{1}{\gamma}} \frac{1}{K} \sum_{k=1}^K [\mathbb{E} [f(\bar{x}_k)] - f^*] \stackrel{(45)}{\leq} \frac{1}{K} \sum_{k=0}^{K-1} \mathbb{E} [\Lambda_k] - \mathbb{E} [\Lambda_{k+1}] = \frac{\Lambda_0 - \mathbb{E} [\Lambda_K]}{K} \leq \frac{\Lambda_0}{K} = \frac{\|x_0 - x_*\|^2}{K}.$$

All that remains is to set $\mu = 0$. □

F Additional plots

To empirically confirm the linear rate of convergence across all settings, we present plots similar to Figure 1 for all runs. Figures 3 and 4 display the convergence of **L-SVRP** for all 48 configurations described in the experimental section, with each figure showing half of the configurations.

Speeding Up Stochastic Proximal Optimization In The High Hessian Dissimilarity Setting

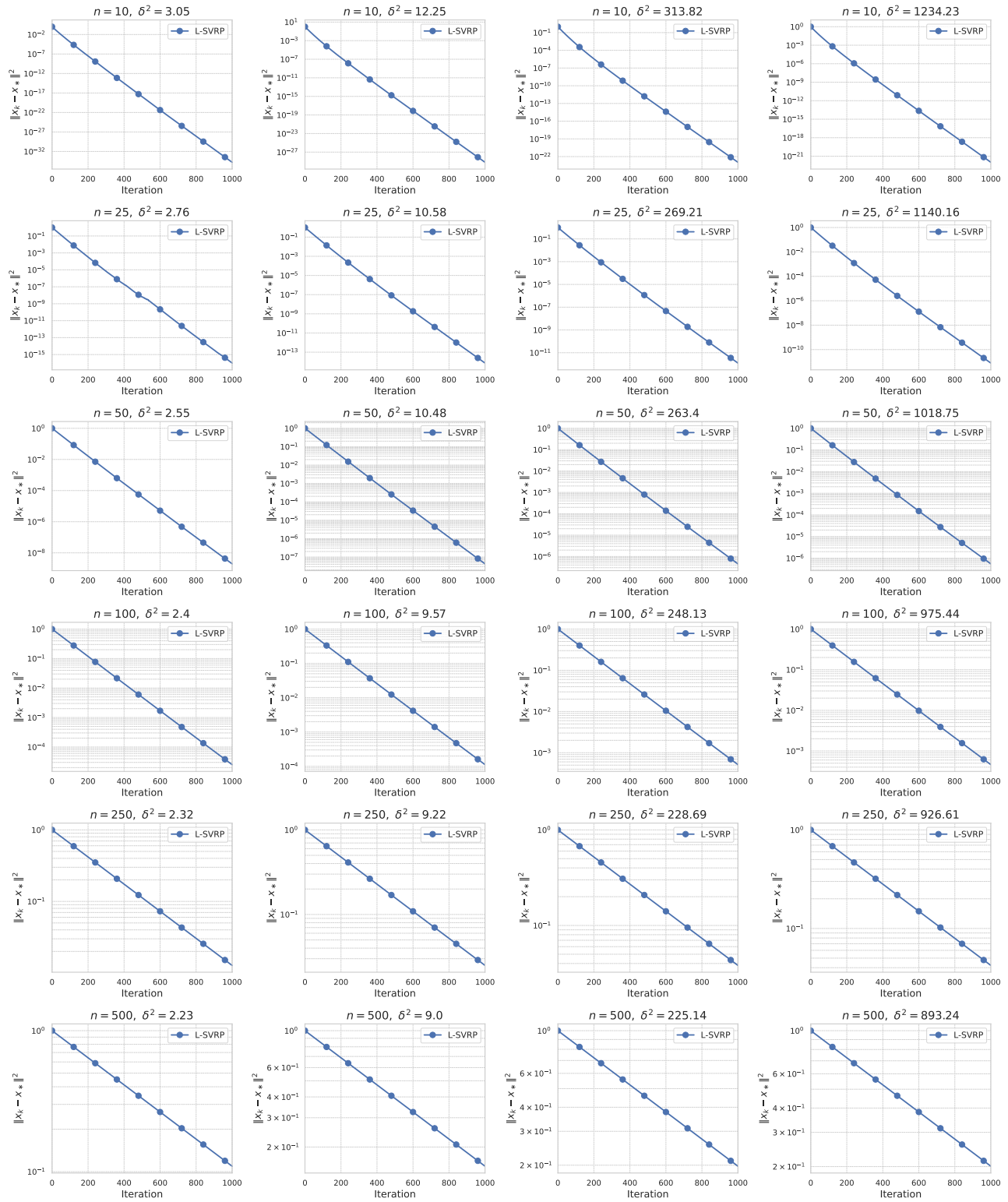


Figure 3: Convergence of L-SVRP for the first half of the 48 configurations described in the experimental section.

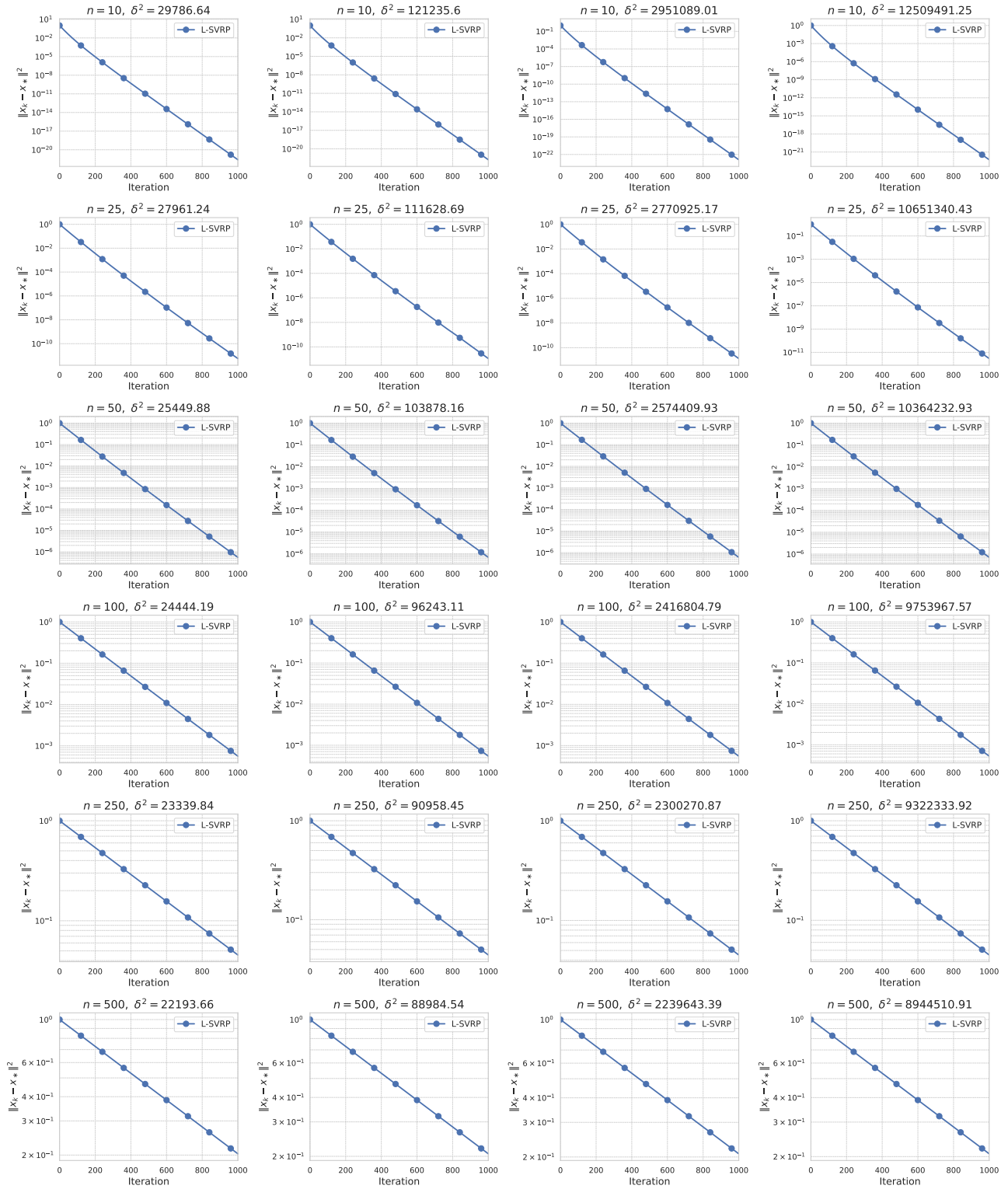


Figure 4: Convergence of L-SVRP for the second half of the 48 configurations described in the experimental section.